

pubs.acs.org/est Article

Emerging Pathogenic Unit of Vesicle-Cloaked Murine Norovirus Clusters is Resistant to Environmental Stresses and UV₂₅₄ Disinfection

Mengyang Zhang, Sourish Ghosh, Manish Kumar, Marianita Santiana, Christopher K. E. Bleck, Natthawan Chaimongkol, Nihal Altan-Bonnet,* and Danmeng Shuai*



Cite This: https://doi.org/10.1021/acs.est.1c01763



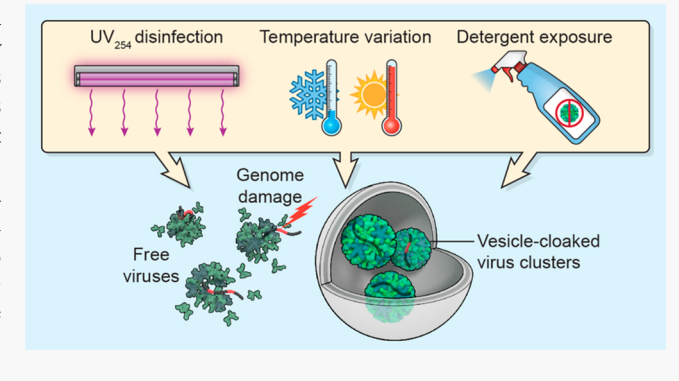
ACCESS

Metrics & More

Article Recommendations

s Supporting Information

ABSTRACT: An individual virion was long believed to act as an independent infectious unit in virology, until the recent discovery of vesicle-cloaked virus clusters which has greatly challenged this central paradigm. Vesicle-cloaked virus clusters (also known as viral vesicles) are phospholipid-bilayer encapsulated fluid sacs that contain multiple virions or multiple copies of viral genomes. Norovirus is a global leading causative agent of gastroenteritis, and the reported prevalence of vesicle-cloaked norovirus clusters in stool has raised concerns whether the current disinfection, sanitation, and hygiene practices can effectively control environmental pollution by these pathogenic units. In this study, we have demonstrated that vesicle-cloaked murine norovirus (MNV-1) clusters were highly persistent under temperature variation (i.e.,



freeze—thaw) and they were partially resistant to detergent decomposition. MNV-1 vesicles were 1.89-3.17-fold more infectious in vitro than their free virus counterparts. Most importantly, MNV-1 vesicles were up to 2.16-times more resistant to UV_{254} disinfection than free MNV-1 at a low viral load in vitro. Interestingly, with the increase of the viral load, free MNV-1 and MNV-1 vesicles showed equivalent resistance to UV_{254} disinfection. We show that the increased multiplicity of infection provided by vesicles is in part responsible for these attributes. Our study, for the first time, sheds light on the environmental behavior of vesicle-cloaked virus clusters as unique emerging pathogenic units. Our study highlights the need to revisit current paradigms of disinfection, sanitation, and hygiene practices for protecting public health.

KEYWORDS: vesicle-cloaked virus clusters, norovirus, environmental stresses, disinfection

INTRODUCTION

Norovirus is a nonenveloped, positive-sense, single-stranded RNA virus from the family of Caliciviridae. Norovirus is the primary cause of epidemic gastroenteritis worldwide across all ages in both healthcare and community settings. Norovirus is estimated to cause 18% of all cases of acute gastroenteritis globally,² with 21 million cases in the U.S. each year.¹ Norovirus is mainly transmitted through the fecal-oral route, with the contribution of water-, food-, and environmentmediated transmission more than direct person-to-person transmission. Several factors promote the transmission and spread of norovirus: a low dose (<100 viral particles) for successful infection, a high shedding concentration in host excreta, a prolonged infectious period of hosts, and high prevalence and persistence in the environment.³ Norovirus shedding in the feces of patients can last 13-56 days, and up to 10¹² virus genome copies per gram of stool can be present.⁴ As a result, norovirus is detected with a high concentration of up to 109 and 106 genome copies L-1 in raw and treated wastewater, respectively. 5,6 Moreover, norovirus is extremely persistent in water and infectious in human volunteers even after being exposed to groundwater at room temperature for 61 days. Although the infectivity of norovirus in treated wastewater has not been established, the detection of norovirus genomes could imply the resistance of norovirus to current wastewater treatment processes. Thus, it is critical to understand norovirus removal and inactivation for further advancing wastewater and water treatment and guaranteeing safe water production and public health protection.

Disinfection has been widely adopted in water and wastewater treatment for inactivating environmental patho-

Received: March 17, 2021 Accepted: March 23, 2021



gens. Previous studies have shown that chemical disinfectants such as chlorine, monochloramine, chlorine dioxide, peracetic acid, and ozone effectively inactivate diverse viruses. 10-12 Ultraviolet (UV) disinfection has become a popular disinfection process for drinking water treatment and water reclamation because it overcomes the limitation of chemical disinfection to minimize disinfection byproduct generation and it is economically feasible. UV irradiation at 254 nm (UV₂₅₄) mainly attacks viral genomes in disinfection, ¹³⁻¹⁵ and a low dose of 25-35 mJ cm⁻² is expected to inactivate human norovirus and its surrogate of murine norovirus up to 4 logs. 16-18 Bacteriophage MS2, feline calicivirus, and Tulane virus were also selected as human norovirus surrogates in disinfection, 10,19-21 since the human norovirus is extremely difficult to culture in cells to date.²² Selecting appropriate surrogates in lab-scale experiments is essential to evaluate the resistance of human norovirus to disinfection in full-scale water and wastewater treatment and associated risks of the virus. Nevertheless, an emerging format of noroviruses, which was first reported in 2018, 23 raises concerns in the efficacy of water and wastewater disinfection.

It was widely accepted that viruses were exclusively individual particles when released from host cells, and cell lysis occurred when nonenveloped viruses such as norovirus were released.^{24,25} However, recent discoveries have challenged this paradigm and revealed that clusters of viruses, including but not limited to norovirus, rotavirus, enteroviruses such as poliovirus, rhinovirus, and the hepatitis A and E viruses, can be packaged and released from their host cells nonlytically in extracellular vesicles. 23,26–28 Vesicle-cloaked virus clusters (also referred to here as viral vesicles) are phospholipid-bilayer encapsulated fluid sacs that comprise multiple virions or multiple copies of viral genomes, and they can be derived from a variety of cellular origins including autophagosomes, multivesicular bodies, and direct budding from the cell plasma membrane. Extracellular vesicle sizes can range from 100 nm to microns, and different viruses exploit specific-sized vesicles derived from specific cellular organelles. Norovirus vesicles are so-called exosomes, which are typically <200 nm in diameter, contain up to 5 virus particles and derive from multivesicular bodies fusing with the cell plasma membrane.23

Extracellular vesicles have been reported with a high stability under a low storage temperature from -80 to 4 °C, ²⁹ and exosomes remained intact for up to 28 days in whole saliva at 4 °C. ³⁰ Notably viral vesicles are persistent to pass through the gastrointestinal tract of mice and a large population of viruses shed in stool are vesicle-cloaked, e.g., vesicle-cloaked rotavirus clusters contribute to up to 45% of the total stool rotavirus population. ²³ Moreover, extracellular vesicles, acting as vehicles of en bloc viral transmission, enhance the multiplicity of infection (MOI) and allow viral recombination or reassortment to take place, both of which increase virus infectivity by enhancing the kinetics of replication in the initial phases of infection and by complementing deleterious mutations among viral progeny. ^{28,31} Furthermore, viral vesicles also enhance virulence by shielding their viral cargo from host antibodies and by actively suppressing immune defenses. ²⁸

Free viruses can also aggregate in the aquatic environment, ^{32,33} and viral aggregates have shown higher resistance to disinfection than nonaggregated viruses. ^{34,35} However, vesicle-cloaked virus clusters are unique pathogenic units compared to viral aggregates as vesicles with viral clusters are released from

the host, ²⁶ they are not susceptible to decomposition *in vivo*, ²³ and they are stable in wastewater (see discussion). In contrast, viral aggregates are induced by specific environmental matrices such as low pH, certain types of salts and certain salt concentrations, or association with organic matter. ^{32,35}

Given the above, vesicle-cloaked virus clusters could be important yet largely overlooked environmental pathogenic units, because they are persistent in vivo, more infectious than free virus counterparts, and distinct from viral aggregates. Moreover, researchers unintentionally assuming their viral population is free viruses rather than a mixture of free and vesicle-cloaked virus clusters in bench-scale disinfection experiments could lead to misleading findings and interpretations. Since vesicle-cloaked virus clusters are prevalent in animal and human excreta that can contaminate water²³ and their potential persistence in wastewater, disinfection of viral vesicles beyond free viruses should be evaluated. Here we show that vesicle-cloaked virus clusters are resistant to destruction under environmental stresses and significantly more resistant to disinfection than free viruses. Our study highlights the environmental importance of vesicle-cloaked virus clusters as an emerging pathogenic unit, and their persistence, increased infectivity, and enhanced resistance to disinfection call for an urgent need to revisit current paradigms of disinfection, sanitation, and hygiene practices for public health protection.

EXPERIMENTAL METHODS

Cells and Virus Stock. As a widely adopted surrogate of human norovirus, 36,37 MNV-1 was used in our study, and the virus was cultured in RAW 264.7 cells (ATCC TIB-71, RRID: CVCL 0493). RAW 264.7 cells were maintained in Dulbecco's modified Eagle's medium (DMEM) supplemented with 10% fetal bovine serum (FBS) and 1% Penicillin-Streptomycin (P/S) and incubated at 37 °C/5% CO₂ until confluence. DMEM and DMEM supplemented with both FBS and P/S are referred as the serum free medium (SFM) and the complete culture medium (CCM), respectively. For MNV-1 stock propagation and enrichment, confluent RAW 264.7 cells were infected with MNV-1 and incubated at 37 °C/5% CO₂ until a significant cytopathic effect (CPE) was observed. Cells were next frozen and thawed for three times; the suspension was centrifuged (1,000 × g, 15 min) to remove cell debris and the supernatant was collected. Multiple rounds of reinfection may be used for virus enrichment. Enriched MNV-1 stock was aliquoted and stored at -80 °C until use.

Isolation of Vesicle-Cloaked MNV-1 Clusters. Viral vesicles were first separated from cell culture and briefly concentrated by ultracentrifugation before purification. Confluent RAW 264.7 cells were infected with MNV-1 stock and incubated at 37 °C/5% CO₂. After 1 h of incubation, the inoculum was removed, and monolayer cells were rinsed with prewarmed SFM for three times before adding back SFM. At 20 h post infection (hpi), only the supernatant was collected. After cell debris was removed by centrifugation at the speed of $5000 \times g$ for 15 min, the supernatant was proceeded to ultracentrifugation at $100\,000 \times g$ for 1 h at 10 °C. MNV-1 containing vesicle pellet was collected and resuspended gently in 1 mL of SFM for further vesicle purification.

The viral vesicle membrane is enriched with phosphatidylserine (PS) which binds strongly with proteins such as Annexin V or TIM4; nevertheless, these proteins do not bind to naked viruses.²⁸ Thus, the viral vesicles can be separated from free viruses by using PS-binding proteins conjugated magnetic beads to achieve a high purity. All MNV-1 containing vesicles used in this study were purified from the vesicle pellet by the MagCapture Exosome Isolation Kit PS (FUJIFILM Wako Pure Chemical, 293–77601), which uses TIM4 coated magnetic beads, following the protocol provided by the manufacturer (see Supporting Information (SI) for details).

To test the impact of treatments on MNV-1 vesicle integrity, MNV-1 vesicles before and after freeze—thaw, buffer lysis (see Lysis of Vesicles), and UV₂₅₄ disinfection were recovered by the TIM4 coated magnetic beads. Only viruses in the intact vesicles were recovered and quantified by reverse transcription-quantitative polymerase chain reaction (RT-qPCR).

Lysis of Vesicles. To determine the stability of viral vesicles and their membrane structure destruction, multiple cycles of freeze-thaw and two kinds of detergents were tested. Purified MNV-1 vesicles isolated from RAW 264.7 cells were frozen on dry ice and thawed at 37 °C, and the freeze-thaw cycle was repeated for up to 20 times. Sodium dodecyl sulfate (SDS) and nonyl phenoxypolyethoxylethanol (NP-40) were used as representatives for ionic and nonionic detergents, respectively. SDS or NP-40 was added to MNV-1 vesicles to get a final concentration of 1 wt % followed by one min of vortex. A nondetergent lysis buffer (Detergent-Free Exosomal Protein Extraction Kit, 101Bio, P201) was also tested and used in the following experiments for free MNV-1 preparation since the nondetergent lysis buffer did not have a significant influence on MNV-1 infectivity based on the integrated cell culture-reverse transcription-quantitative polymerase chain reaction (ICC-RT-qPCR) analysis (Figure S1). For the treatment with nondetergent lysis buffer, an equivalent volume of lysis buffer A from the Detergent-Free Exosomal Protein Extraction Kit was first added to prechilled MNV-1 vesicles and the mixture was vortexed for 15 s. After quick spin-down, lysis buffer B from the kit was used to neutralize the lysis by another 15 s of vortex. All the lysed MNV-1 vesicles, with untreated MNV-1 vesicles as a control, were then centrifuged at 14 000 rpm at 10 °C for 10 min. The supernatant was collected and diluted to a final volume of 1 mL for particle size measurements.

Measurement of the Particle Size and Concentration of Viral Vesicles. The hydrodynamic size distribution and concentration of lysed and untreated MNV-1 vesicles were measured by NanoSight NS300 (Malvern Panalytical) following the manufacturer's specifications. Before or between sample measurement, double-distilled water (ddH₂O) was always applied to check the background signal and rinse tubing. During the measurement, all the settings, including flow rate, screen gain, camera level, and detection threshold, were kept the same to ensure that the results of different samples were comparable. D-values that illustrate statistical particle size distribution were also determined, and D10, D50, and D90 reflect the particle diameter which 10%, 50%, and 90% of the population lies below.

UV₂₅₄ Disinfection. UV₂₅₄ disinfection was carried out with a Spectrolinker XL-1500 UV Cross-linker (Spectronics Corporation), which was precalibrated and offered controllable UV₂₅₄ dosages (0–50 mJ cm⁻²). MNV-1 vesicles were divided into two equal fractions with one fraction left intact and the other fraction lysed with the Detergent-Free Exosomal Protein Extraction Kit to release free MNV-1 particles. Since lysis buffer addition increased the volume of free MNV-1, an equal volume of phosphate-buffered saline (PBS) was amended to the MNV-1 vesicles to compensate the volume increase in free

MNV-1. Therefore, MNV-1 vesicles and free MNV-1 used for disinfection had the same genome concentration (Figure S2). Details of UV_{254} exposure were included in the next section. During disinfection, samples were withdrawn at a series of UV_{254} doses and proceeded to ICC-RT-qPCR immediately for determining the infectivity.

The \log_{10} reduction of the infectivity of MNV-1 vesicles and free MNV-1 after exposure to UV₂₅₄ irradiation was calculated using the following equation:

$$Log_{10} \text{ inactivation} = -log_{10} \left(\frac{N_t}{N_0} \right)$$
 (1)

where N_t and N_0 are the genome copy number per well of UV₂₅₄-treated and untreated viruses as measured by ICC-RT-qPCR, respectively. Details of ICC-RT-qPCR are included in a following section. The first-order inactivation rate constant was obtained as 2.303 (= ln10) times the slope of the linear regression of \log_{10} inactivation versus UV₂₅₄ dosage.

Calibration of UV₂₅₄ **Exposure.** Since different solutions have different light absorption due to their unique impurities, calibration was applied to estimate more precise UV_{254} exposure on MNV-1 vesicles and free MNV-1. UV_{254} irradiation in different solutions was calibrated mathematically following the Beer–Lambert Law:³⁸

$$UVT = \frac{I}{I_0} = 10^{-A}$$
 (2)

$$A = \sum \varepsilon lc \tag{3}$$

where UVT is the UV₂₅₄ transmittance, I is the intensity of UV₂₅₄ transmitted through the sample (mW cm⁻²), I_0 is the intensity of UV₂₅₄ incident on the sample (mW cm⁻²), A is UV₂₅₄ absorbance at a specific path length, ε is the molar absorption coefficient of a solute (M⁻¹ cm⁻¹), ε is molar concentration of a solute (M), and l is the path length or the solution height (cm).

The UV_{254} absorbance through the background of MNV-1 vesicle and free MNV-1 solutions was measured by NanoDrop (ThermoFisher Scientific Inc.) and the microvolume measurement was normalized to an equivalent path length of 1 cm. The UV_{254} absorbance for each sample and mathematical calculations for estimating UV_{254} exposure to the viruses in disinfection are shown in Table S1.

ICC-RT-qPCR Assay. The presence of vesicle-cloaked virus clusters challenges many traditional quantitative methods for enumerating infectious viruses, such as plaque and focus forming assay and the most probable number assay, which are built upon the assumption of single virion infection. ICC-RT-qPCR overcomes the limitation and provides a rapid, sensitive, and reliable quantitative measurement of viral infectivity, using RT-qPCR to determine the number of viral genes produced during virus replication in the host cells. In addition, the amount of inoculum used for an ICC-RT-qPCR assay could be largely reduced, which saves precious samples of viral vesicles. Special attention should be paid that ICC-RT-qPCR could overestimate the dosage of disinfectants to achieve desired performance for inactivating viruses compared to a conventional cell culture assay.

A 96-well plate was used to minimize the amount of MNV-1 vesicles and free MNV-1 required for getting a quantifiable PCR signal in the infectivity test. To optimize ICC-RT-qPCR performance, the growth curves of MNV-1 vesicles were

evaluated (Figures S3 and S4) to determine the incubation time for virus binding/entry and propagation. MNV-1 vesicles and free MNV-1 were introduced to the RAW 264.7 cells and incubated for 4 h to allow efficient virus binding/entry but not significant replication, and then the inoculum was removed, and the cells were rinsed by prewarmed SFM for three times. $100~\mu\text{L}$ of fresh SFM was next added into each well and the cells were incubated for another 20 h until ready for RNA extraction. After 24 h of incubation in total, the supernatant in the cell culture was removed and viral RNA was isolated from cell lysate by using the MagMAX-96 Viral RNA Isolation Kit (Thermo Fisher Scientific Inc., AM1836). The RNA in the elution buffer was stored at $-80~^{\circ}\text{C}$ until proceeded to RT-qPCR.

RT-qPCR was conducted using the TaqMan Fast Virus 1-Step Master Mix kit (Thermo Fisher Scientific Inc., 4444432), which combines reverse transcription (RT) reaction with quantitative PCR together. Each 20 µL of reaction mix contained 5 µL of RNA template, 5 µL of Fast Virus Master Mix, 2 μ L of forward primer (10 μ M), 2 μ L of reverse primer (10 μ M), 1.25 μ L of probe, and 4.75 μ L of RNA-free water. The hydrolysis probes were applied for detection, which consisted of the fluorescein (FAM), i.e., a fluorescent reporter, at the 5' end and the Black Hole Quencher 1 dye (BHQ1), i.e., a quencher, at the 3' end. The absolute genome copy numbers were standardized using a series of 10-fold dilutions (10³-10¹⁰ copies mL⁻¹) of synthetic cDNA oligos.^{23,41} Detailed sequence information is listed in Table S2. The RT-qPCR program was run on the Applied Biosystems 7900HT instrument: reverse transcription (52 °C for 10 min), reverse transcription inactivation and denaturation initiation (95 °C for 20 s), and 45 cycles of amplification (95 $^{\circ}$ C for 15 s and 60 $^{\circ}$ C for 60 s). RNA-free water was used as the negative control. qPCR efficiency for MNV-1 was 90.8-106.3% and its coefficient of determination was 0.998-1 (Table S3). Serial dilutions of extracted RNA from MNV-1 did not indicate any inhibition for qPCR (Table S4). All the RT-qPCR data were reported following MIQE guidelines.42

A linear correlation was observed between virus infectivity determined by ICC-RT-qPCR and the viral load before infection quantified by RT-qPCR, for both MNV-1 stock and MNV-1 vesicles with serial dilutions (Figures S5 and S6), highlighting the validity of ICC-RT-qPCR for quantifying the virus infectivity. Twenty-four h of incubation in the RAW 264.7 cells was effective for accurately determining MNV-1 infectivity with different viral loads. Special attention should be paid that the MNV-1 genome input was measured by RT-qPCR and it did not represent the infectious MNV-1 concentration. The viral load and infectivity of MNV-1 vesicles used in the infectivity and disinfection studies fell in the linear range in Figure S6.

Immune Electron Microscopy (Immuno-EM) of Viral Vesicles. Immunostaining was conducted to confirm that the vesicles contained MNV-1. MNV-1 vesicles were loaded onto glow discharged carbon coated copper grids (CF400-Cu, Electron Microscopy Sciences), followed by fixation with 4% formaldehyde and 1% glutaraldehyde in PHEM buffer for 10 min and quenching in 0.15% glycine in PBS. Immunolabeling was performed by incubating grids with a primary rabbit polyclonal antibody UM656 to MNV-1 (a gift from Dr. Christiane Wobus, University of Michigan, Ann Arbor) at 1:10 dilution in 2% bovine serum albumin (BSA) in PBS for 2 h, followed by incubation with 5 nm protein A gold (UMC

Utrecht University, Utrecht, Netherlands, 1:50 dilution) for 1 h. Grids were then postfixed in 1% glutaraldehyde in PBS for 5 min, washed three times with ddH_2O , and negatively stained with NanoVan (Nanoprobes Inc., 14701). Grids were examined with a JEM-1200EX (JEOL, U.S.A.) transmission electron microscope (TEM, accelerating voltage 80 keV) equipped with a bottom-mounted AMT 6-megapixel digital camera (Advanced Microscopy Techniques Corp, U.S.A.).

Statistical Analysis. Unpaired Student's t test was applied for the statistical comparison between MNV-1 vesicles and free MNV-1 regarding infectivity and particle size distribution analysis, which returned to a p value. UV₂₅₄ inactivation rate constants for MNV-1 vesicles and free MNV-1 were statistically compared by following a two-tailed Student's distribution test, which also returned to a p value. All p values <0.05 were considered statistically significant.

RESULTS

Vesicle-Cloaked Murine Norovirus Clusters Are Persistent under Exposure to Selected Environmental Stresses. We isolated vesicle-cloaked MNV-1 clusters from MNV-1 infected RAW 264.7 cells, a mouse macrophage cell line, as described in the methods. Isolated vesicles contained multiple MNV-1 particles per vesicle (up to 5 per vesicle as previously reported²³), and these viral particles could be labeled with an antibody against the MNV-1 capsid and imaged with immuno-EM (Figure 1).

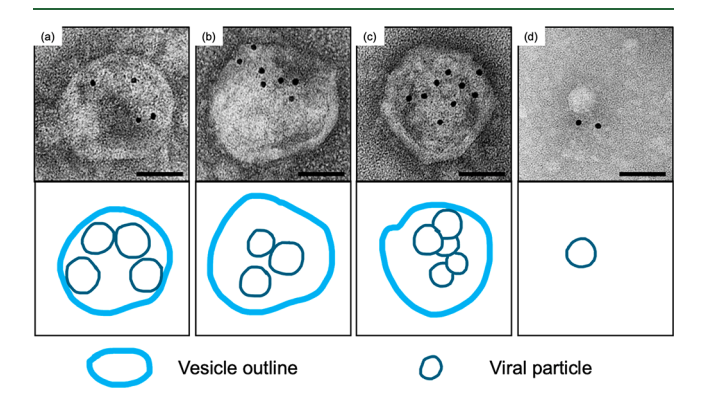


Figure 1. Immuno-EM of MNV-1 vesicles (a-c) and free MNV-1 (d) as a positive control. Scale bars are 50 nm.

Multiple freeze-thaw cycles are one of the most common approaches to disrupt membrane-bound vesicles and release free viruses. 26,43 We first interrogated whether the isolated MNV-1 vesicles would remain intact after multiple cycles of freeze-thaw. As shown in Figure 2a and Table S5, the hydrodynamic diameter of viral vesicles was maintained at an average of ca. 185 nm and did not show any significant change even after 20 cycles of freeze-thaw (184.9 \pm 64.7 nm before freeze-thaw, and 186.8 \pm 63.1 and 188.5 \pm 63.7 nm after 10 and 20 freeze-thaw cycles, respectively). D10 (ca. 128 nm), D50 (ca. 170 nm), and D90 (ca. 265 nm) also did not shift apparently when compared with those of viral vesicles before freeze-thaw (for all comparisons p > 0.05). The D-values indicated that the size of 80% of MNV-1 vesicles fell in the range of 128-265 nm. The particle concentration also did not decrease statistically after up to 20 cycles of freeze-thaw, and it supports the argument that MNV-1 vesicles did not decompose significantly (5.62 \pm 0.55 \times 10⁸ particles mL⁻¹

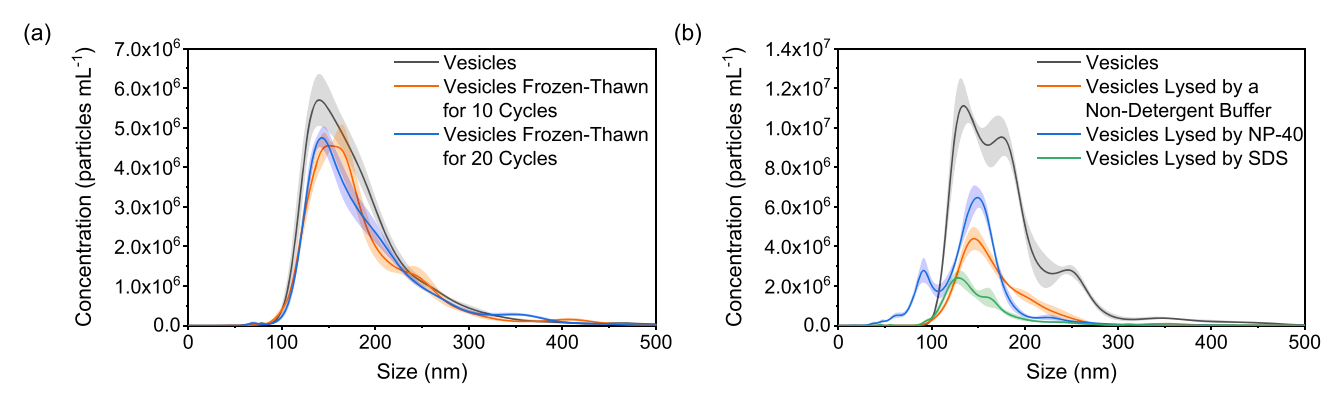


Figure 2. Hydrodynamic size distribution of vesicle-cloaked MNV-1 clusters before and after (a) multiple cycles of freeze—thaw and (b) the treatment by detergents (1 wt % NP-40 or 1 wt % SDS) and a nondetergent lysis buffer (Detergent-Free Exosomal Protein Extraction Kit). Error bars represent standard errors for 3–5 replicates.

before freeze—thaw, and $4.47 \pm 0.29 \times 10^8$ and $4.45 \pm 0.23 \times 10^8$ particles mL⁻¹ after 10 and 20 freeze—thaw cycles, respectively, p > 0.05). MNV-1 vesicles before and after 20 cycles of freeze—thaw were also recovered by using TIM4 coated magnetic beads, and RT-qPCR quantification indicated that the treatment did not reduce recovery (Figure S7). Note that TIM4 selectively binds PS on the vesicle membranes but not free MNV-1,²³ and thus only MNV-1 in intact vesicles were harvested and quantified. The result also highlighted that MNV-1 vesicles did not decompose in freeze—thaw. Overall, MNV-1 vesicles showed significant resistance to temperature variation, i.e., multiple freeze—thaw cycles.

Detergents are widely used disinfectants for inactivating viruses, especially enveloped viruses by destructing the lipid layer of the viruses. In addition, detergents are also common for household cleaning and they are ubiquitously present in municipal wastewater. Therefore, we next evaluated whether detergents could destabilize MNV-1 vesicles. We tested MNV-1 vesicle stability under the treatment of two detergents, SDS and NP-40 as a representative ionic and nonionic detergent, respectively. The detergent concentration of 1 wt % and the treatment duration of 1 min were applied for both experiments with SDS and NP-40, which were reported as effective disinfectants for enveloped viruses like influenza and severe acute respiratory syndrome coronavirus (SARS-CoV). 44,45 In addition, a proprietary commercial kit, i.e., Detergent-Free Exosomal Protein Extraction Kit, was also used to test the effect of a nondetergent lysis buffer for decomposing the MNV-1 vesicles. As shown in Figure 2b and Table S6, there was no significant change of the vesicle size but a remarkable decrease of the vesicle concentration for samples treated by SDS, NP-40, and the nondetergent lysis buffer. NanoSight NS300 uses the nanoparticle tracking analysis, which determines the hydrodynamic diameter of a particle based on light scattering and Brownian motion. The detection limit of NanoSight NS300 is 50-70 nm. 46,47 Although, free MNV-1 with an individual virion size of ca. 30 nm cannot be characterized by NanoSight NS300, the decrease in the concentration of vesicles >70 nm indicates vesicle lysis. Among all three treatments, SDS destroyed the most MNV-1 vesicles, with only 14.2% of vesicles remaining after exposure to SDS, while 39.5% and 29.0% of MNV-1 vesicles were detected after being treated with NP-40 and the nondetergent lysis buffer, respectively.

We also used RT-qPCR to measure viral genomic RNA content of MNV-1 vesicles recovered with TIM4 magnetic

beads before and after nondetergent lysis buffer treatment. We found that only 38.2% of MNV-1 remained in the intact vesicles after treatment (Figure S8). This result supports the data obtained from the dynamic light scattering characterization and indicates that nondetergent lysis buffer is an effective treatment to obtain free MNV-1 for use in the infectivity and disinfection studies below.

Vesicle-Cloaked Murine Norovirus Clusters Are More Infectious than Free Murine Noroviruses. The infectivity of vesicle-cloaked MNV-1 clusters for cell culture was investigated and compared with that of free MNV-1 by ICC-RT-qPCR. MNV-1 vesicles were divided into two equal fractions with one fraction left intact and the other fraction lysed with the nondetergent buffer to release free MNV-1 particles. Note that each fraction contained the same quantity of MNV-1 (Figure S2), and the lysis buffer, which was effective as described above (Figures 2b and S8), did not adversely impact the infectivity of the free virus population (Figure S1). As shown in Figure 3, the vesicle-cloaked MNV-1 clusters showed significant higher infectivity than their free virus counterpart in RAW 264.7 cells (i.e., 1.89-3.17-times more infectious, for all comparations p < 0.05), and this phenomenon was consistent for all batches of MNV-1 vesicles and all virus loads that were tested.

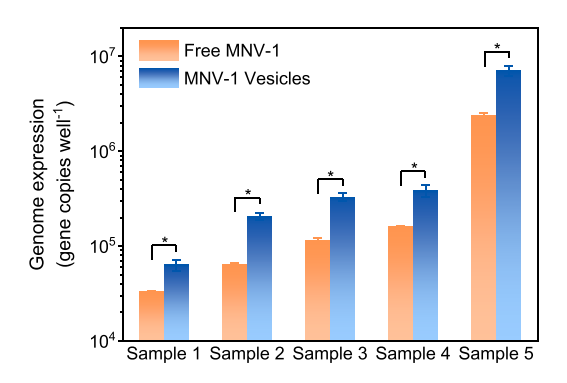


Figure 3. Vesicle-cloaked MNV-1 clusters are more infectious than free MNV-1. Samples 1, 2, and 3 were MNV-1 vesicles isolated on 01/17/20 with an inoculum volume of 2, 5, and 10 μ L, respectively. Samples 4 and 5 were MNV-1 vesicles isolated on 01/30/20 and 02/18/20 with an inoculum volume of 2 μ L, respectively. n = 4, and error bars represent standard deviations. *p < 0.05.

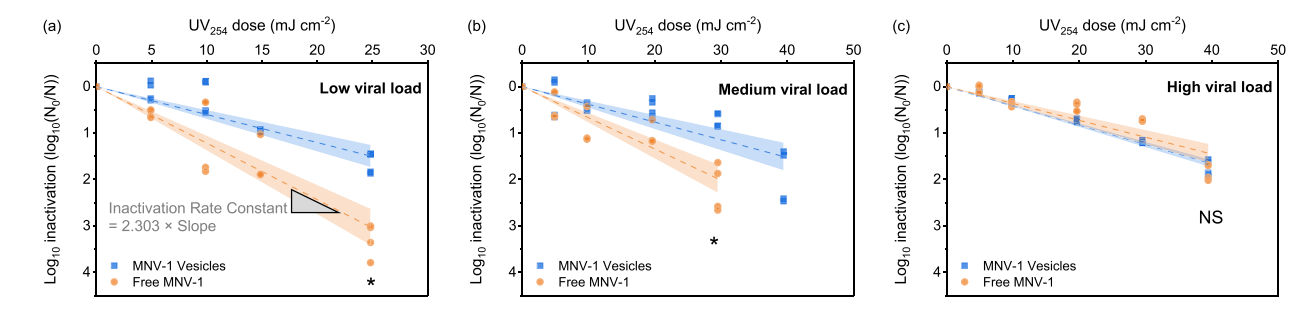


Figure 4. UV₂₅₄ disinfection for MNV-1 vesicles and free MNV-1 of a low (a), medium (b), and high (c) viral load. MNV-1 vesicles are more resistant to UV₂₅₄ disinfection than free MNV-1 at the low and medium viral loads. Statistical significance was compared between the inactivation rate constant of MNV-1 vesicles and free MNV-1. For the low, medium, and high viral load, the infectivity of MNV-1 vesicles in the inoculum before UV₂₅₄ treatment was 1.06×10^4 , 1.02×10^5 , and 1.60×10^7 gene copies well⁻¹, respectively. MNV-1 vesicles and free MNV-1 were suspended in the elution buffer plus PBS and the elution buffer plus the nondetergent lysis buffer, respectively. n = 4, 95% confidence limits are shown in light blue and orange, and * p < 0.05 and NS p > 0.05.

Vesicle-Cloaked Murine Norovirus Clusters Are More Resistant to UV₂₅₄ Disinfection than Free Murine **Noroviruses.** Log₁₀ inactivation of vesicle-cloaked MNV-1 clusters in UV₂₅₄ disinfection were evaluated and compared with that of free MNV-1 in Figure 4. The nondetergent lysis buffer was selected to release free MNV-1 from MNV-1 vesicles, and MNV-1 vesicles and free MNV-1 from the same batch with the same viral load (Figure S2) were used. The UV₂₅₄ dosage was calibrated by considering the shielding effect of the reaction solution (Table S1). As shown in Figure 4a, the vesicle-cloaked MNV-1 clusters were significantly more resistant to UV₂₅₄ disinfection than free MNV-1: the inactivation rate constant for MNV-1 vesicles and free MNV-1 was 0.139 and 0.300 cm² mJ⁻¹ (p < 0.05), respectively. The initial viral load and corresponding infectivity of this batch of MNV-1 vesicles before disinfection was low, and the viral vesicles propagated in the RAW 264.7 cells for 24 h and produced 1.06×10^4 gene copies of MNV-1 per well in a 96well plate. Interestingly, with the increase of the initial viral load of the MNV-1 vesicles (and thereby increase of free viruses), the difference of resistance to UV₂₅₄ disinfection between viral vesicles and free viruses was less apparent. The inactivation rate constants for MNV-1 vesicles and free MNV-1 were 8.80×10^{-2} and $0.181 \text{ cm}^2 \text{ mJ}^{-1}$ (p < 0.05), respectively, when the initial infectivity of MNV-1 vesicles was 1.02×10^5 gene copies well-1 (Figure 4b); and the inactivation rate constants for MNV-1 vesicles and free MNV-1 were statistically the same $(9.58 \times 10^{-2} \text{ versus } 9.51 \times 10^{-2} \text{ cm}^2 \text{ mJ}^{-1}, p >$ 0.05) when the initial infectivity of MNV-1 vesicles reached to 1.60×10^7 gene copies well⁻¹ (Figure 4c). To conclude, MNV-1 vesicles are up to 2.16-times more resistant to UV₂₅₄ disinfection than free MNV-1, when the viral load to host cells was low, and with the increase of the virus load, free MNV-1 and MNV-1 vesicles showed equivalent resistance to UV₂₅₄ disinfection.

The morphology of MNV-1 vesicles before and after UV₂₅₄ treatment was monitored by TEM (Figure S9). There was no significant difference in the size or morphology of viral vesicles before and after 40 mJ cm⁻² of UV₂₅₄ irradiation. Special attention should be paid because vesicles could break up in TEM sample preparation and the number of broken vesicles could be overestimated compared to that in physiological conditions. More quantitative characterizations of MNV-1 vesicles before and after UV₂₅₄ treatment were conducted by recovery and nanoparticle tracking analysis. MNV-1 vesicles

before and after 40 mJ cm $^{-2}$ of UV $_{254}$ irradiation were recovered by TIM4 coated magnetic beads and quantified by RT-qPCR. The equivalent recovery for both samples (Figure S10) indicated MNV-1 vesicle membranes remained intact upon 40 mJ cm $^{-2}$ of UV $_{254}$ exposure. Quantitative size distribution of MNV-1 vesicles before and after UV $_{254}$ treatment was measured by NanoSight NS300 (Figure S11, Table S7), and the size distribution of viral vesicles did not vary statistically after the exposure to UV $_{254}$ irradiation up to 40 mJ cm $^{-2}$. The particle concentration of viral vesicles was $5.10\pm0.28\times10^7$ particles mL $^{-1}$ before treatment and $5.33\pm0.57\times10^7$ and $4.79\pm0.60\times10^7$ particles mL $^{-1}$ after exposure to 25 and 40 mJ cm $^{-2}$ of UV $_{254}$ irradiation, respectively (p>0.05). Given all of the above, UV $_{254}$ disinfection did not compromise the integrity of MNV-1 vesicles.

DISCUSSION

The persistence of viral vesicles under environmental stresses like temperature variation and detergent treatment highlights the environmental importance of this emerging pathogenic unit, because they could be ubiquitously present and persist in wastewater and natural water, and many other environments contaminated with animal or human excreta. Indeed, we have found that vesicles containing rotavirus clusters harvested from stool, can remain intact in raw wastewater and nearly 60% of these vesicles can be recovered after 7 days (Figure S12). Our finding regarding freeze-thaw cycles not decomposing viral vesicles is notable because it can complicate the interpretation of results from previous viral disinfection studies, 39,48 which were not aware of the presence and contribution of such vesicles. Chemical treatment by detergents or lysis buffers may be needed beyond freezing and thawing to get free viruses with a higher purity from the cell culture.

We also reported here that viral vesicles are partially resistant to chemical treatment by detergents and the nondetergent lysis buffer. Cholesterol and sphingomyelin are known critical lipid components which facilitate plasma membrane integrity during freeze—thaw cycles and detergent treatment. Consistent with this, lipidomic analysis of MNV-1 exosomes has shown up to 3-fold enrichment of cholesterol and sphingomyelin. Thus, the viral vesicle membrane may provide an extra barrier of protection for viruses from detergent inactivation, (Figure 5a). Partial resistance of MNV-1 vesicles to detergent destruction may suggest they remain infectious, in the form of vesicle-contained or free nonenveloped viruses.

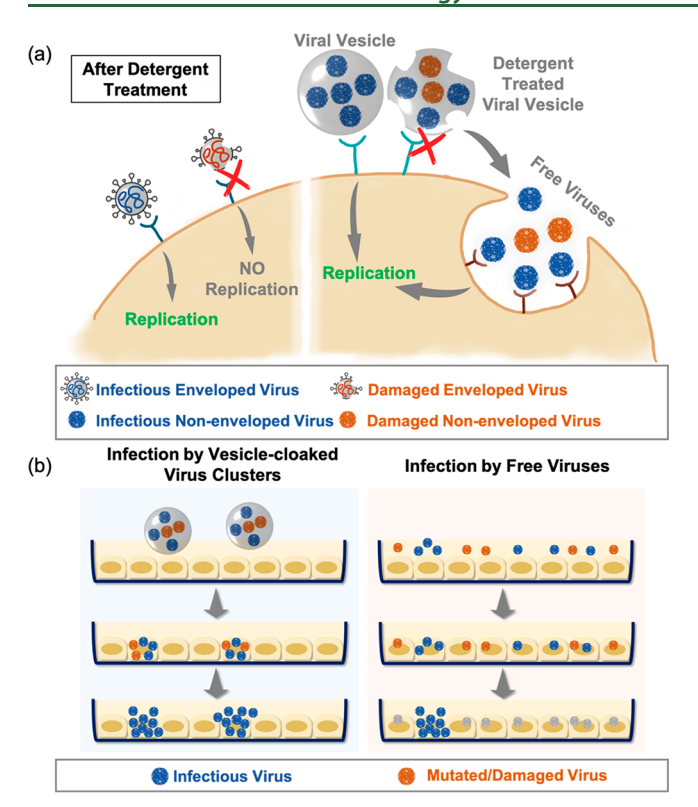


Figure 5. (a) Viral vesicles are more resistant to detergent inactivation than enveloped viruses. (b) Viral vesicles increase MOI.

enveloped viruses like coronavirus are highly susceptible to detergent inactivation, 44,45 because they lose fusion capability with host membranes after envelope destruction which is required for the delivery of their genetic material into the host cytoplasm.

Finally, we found that viral vesicles did not behave like free viruses under UV₂₅₄ exposure: they retained more of their infectivity. The en bloc transmission of viral particles is known to increase MOI (Figure 5b), 23,26,28 which enhances replication kinetics since the host cell takes up multiple viral particles simultaneously in a vesicle. As it was shown for poliovirus, when few viral particles enter a cell, replication is not successful.²⁶ This may be due to individual viral genomes not producing enough viral proteins to begin replication before host defenses kick in and/or individual genomes carrying mutations or lesions that attenuate their replication, the latter becoming corrected by complementary interactions taking place among multiple entering genomes. 28,52 Given this, it is likely that the reason why vesicles containing MNV-1 retained infectivity after UV₂₅₄ exposure is that by entering cells en bloc, the mutated or damaged viruses were still able to cooperate and complement each other's deficiencies to replicate. In contrast when free viruses were damaged with UV₂₅₄, they entered cells alone or in low numbers and were not able to sufficiently cooperate or complement each other's deficiencies to replicate. Thus, only when we increased the free virus loads did we observe an equivalent resistance to UV_{254} disinfection as with virus delivery by vesicles.

■ ENVIRONMENTAL IMPLICATIONS

Our work highlights the environmental and public health importance of viral vesicles as an emerging pathogenic unit, because they could be ubiquitously present and persist in the environment, e.g., water, air, food, and contact surfaces. Specifically, at low environmentally relevant viral loads, the fact that virus vesicles are more resistant to disinfection than free viruses challenges the efficacy and safety of the current paradigm of disinfection, sanitation, and hygiene practices. A combination of multiple disinfectants or an increased disinfectant dose will likely be required to fully inactivate the viral vesicles.

Beyond norovirus, many other environmentally relevant viruses like rotavirus, enterovirus A71, coxsackievirus, poliovirus, rhinovirus, and hepatitis A and E viruses, all transmit en bloc inside vesicles. Especially for coxsackievirus, poliovirus, and rotavirus, more than 25 viral particles can be carried in a single vesicle that allow a significantly increased MOI in infection.²⁸ Notably extracellular vesicles may not only contain complete virions but also free viral genomes and proteins as well as cellular lipids, proteins, and nucleic acids (e.g., mRNA and miRNA), which could modulate infection.²⁸ The presence of viral vesicles in water, air, food, built environment, and other environmental settings should be explored and their resistance to environmental stresses and disinfection should also be comprehensively investigated in the future, which will provide rigorous guidelines for environmental pathogen control and public health protection.

ASSOCIATED CONTENT

Supporting Information

The Supporting Information is available free of charge at https://pubs.acs.org/doi/10.1021/acs.est.1c01763.

Isolation of MNV-1 vesicles using MagCapture Exosome Isolation Kit PS; transmission electron microscopy (TEM) of viral vesicles; vesicle-cloaked rotavirus clusters were persistent in raw wastewater; Table S1, calibration of UV₂₅₄ exposure in disinfection; Table S2, sequence information used in RT-qPCR; Table S3, summary of qPCR assay efficiencies and R2 of standard curve regression; Table S4, RT-qPCR quantification of undiluted and diluted extracted viral RNA; Table S5, summary of particle size and concentration of MNV-1 vesicles after multiple cycles of freeze-thaw; Table S6, summary of particle size and concentration of MNV-1 vesicles after treatment with detergents and a nondetergent lysis buffer; Table S7, summary of particle size and concentration of MNV-1 vesicles after UV₂₅₄ irradiation; Figure S1, non-detergent lysis buffer did not influence the infectivity of MNV-1; Figure S2, genome concentration of MNV-1 vesicles and free MNV-1 lysed from the same batch and the same amount of vesicles; Figure S3, growth curve of MNV-1 vesicles in RAW 264.7 cells without inoculum removal; Figure S4, growth curve of MNV-1 vesicles in RAW 264.7 cells; Figure S5, linear correlation of the infectivity of MNV-1 stock with the viral load before infection; Figure S6, linear correlation of the infectivity of MNV-1 vesicles with the viral load before infection; Figure S7, recovery of MNV-1 vesicles before and after 20 cycles of freezethaw; Figure S8, recovery of MNV-1 vesicles before and after treatment by a non-detergent lysis buffer; Figure S9, characterizations of vesicle-cloaked MNV-1 clusters; Figure S10, recovery of MNV-1 vesicles; Figure S11, hydrodynamic size distribution of MNV-1 vesicles before and after UV₂₅₄ disinfection; Figure S12, Western

blot for rotavirus vesicles after incubation with filtered raw wastewater and quantification of VP6 protein levels of rotavirus by Western blot; and additional references (PDF)

AUTHOR INFORMATION

Corresponding Authors

Nihal Altan-Bonnet — Laboratory of Host—Pathogen Dynamics, National Heart Lung and Blood Institute, National Institutes of Health, Bethesda, Maryland 20892, United States; Phone: 301-435-0817; Email: nihal.altan-bonnet@nih.gov; https://www.nhlbi.nih.gov/science/host-pathogen-dynamics

Danmeng Shuai — Department of Civil and Environmental Engineering, The George Washington University, Washington, District of Columbia 20052, United States; Orcid.org/0000-0003-3817-4092; Phone: 202-994-0506; Email: danmengshuai@gwu.edu; Fax: 202-994-0127; http://materwatersus.weebly.com

Authors

Mengyang Zhang — Department of Civil and Environmental Engineering, The George Washington University, Washington, District of Columbia 20052, United States; Laboratory of Host—Pathogen Dynamics, National Heart Lung and Blood Institute, National Institutes of Health, Bethesda, Maryland 20892, United States

Sourish Ghosh – Laboratory of Host–Pathogen Dynamics, National Heart Lung and Blood Institute, National Institutes of Health, Bethesda, Maryland 20892, United States

Manish Kumar – Laboratory of Host–Pathogen Dynamics, National Heart Lung and Blood Institute, National Institutes of Health, Bethesda, Maryland 20892, United States

Marianita Santiana – Laboratory of Host–Pathogen Dynamics, National Heart Lung and Blood Institute, National Institutes of Health, Bethesda, Maryland 20892, United States

Christopher K. E. Bleck – Electron Microcopy Core, National Heart Lung and Blood Institute, National Institutes of Health, Bethesda, Maryland 20892, United States

Natthawan Chaimongkol – Laboratory of Infectious Diseases, National Institute of Allergy and Infectious Diseases, National Institutes of Health, Bethesda, Maryland 20892, United States

Complete contact information is available at: https://pubs.acs.org/10.1021/acs.est.1c01763

Notes

The authors declare no competing financial interest.

■ ACKNOWLEDGMENTS

We thank NSF Grant (CBET-2028464) and University Facilitating Fund at The George Washington University for supporting our research. We thank NHLBI and NIAID Intramural Research Programs for supporting our work. We thank Dr. Christiane Wobus from University of Michigan Medical School for kindly providing MNV-1 antibody of UM656. We also thank Dr. Ye Sun, from the Electron Microscopy Core Facility at the NHLBI, for assisting the TEM analysis.

■ REFERENCES

- (1) Robilotti, E.; Deresinski, S.; Pinsky, B. A. Norovirus. Clin. Microbiol. Rev. 2015, 28 (1), 134–164.
- (2) Ahmed, S. M.; Hall, A. J.; Robinson, A. E.; Verhoef, L.; Premkumar, P.; Parashar, U. D.; Koopmans, M.; Lopman, B. A. Global prevalence of norovirus in cases of gastroenteritis: a systematic review and meta-analysis. *Lancet Infect. Dis.* **2014**, *14* (8), 725–730.
- (3) Lopman, B.; Gastanaduy, P.; Park, G. W.; Hall, A. J.; Parashar, U. D.; Vinje, J. Environmental transmission of norovirus gastroenteritis. *Curr. Opin. Virol.* **2012**, *2* (1), 96–102.
- (4) Atmar, R. L.; Opekun, A. R.; Gilger, M. A.; Estes, M. K.; Crawford, S. E.; Neill, F. H.; Graham, D. Y. Norwalk virus shedding after experimental human infection. *Emerging Infect. Dis.* **2008**, *14* (10), 1553–1557.
- (5) Da Silva, A. K.; Le Saux, J. C.; Parnaudeau, S.; Pommepuy, M.; Elimelech, M.; Le Guyader, F. S. Evaluation of removal of noroviruses during wastewater treatment, using real-time reverse transcription-PCR: different behaviors of genogroups I and II. *Appl. Environ. Microbiol.* **2007**, 73 (24), 7891–7897.
- (6) La Rosa, G.; Pourshaban, M.; Iaconelli, M.; Muscillo, M. Quantitative real-time PCR of enteric viruses in influent and effluent samples from wastewater treatment plants in Italy. *Ann. Ist Super Sanita* **2010**, 46 (3), 266–273.
- (7) Seitz, S. R.; Leon, J. S.; Schwab, K. J.; Lyon, G. M.; Dowd, M.; McDaniels, M.; Abdulhafid, G.; Fernandez, M. L.; Lindesmith, L. C.; Baric, R. S.; Moe, C. L. Norovirus infectivity in humans and persistence in water. *Appl. Environ. Microbiol.* **2011**, 77 (19), 6884–6888.
- (8) Campos, C. J. A.; Avant, J.; Lowther, J.; Till, D.; Lees, D. N. Human norovirus in untreated sewage and effluents from primary, secondary and tertiary treatment processes. *Water Res.* **2016**, *103*, 224–232.
- (9) Campos, C. J. A.; Avant, J.; Lowther, J.; Till, D.; Lees, D. Levels of norovirus and *E. coli* in untreated, biologically treated and UV-disinfected sewage effluent discharged to a shellfish water. *J. Water Resour. Prot.* **2013**, *05* (10), 978–982.
- (10) Rachmadi, A. T.; Kitajima, M.; Kato, T.; Kato, H.; Okabe, S.; Sano, D. Required chlorination doses to fulfill the credit value for disinfection of enteric viruses in water: a critical review. *Environ. Sci. Technol.* **2020**, *54* (4), 2068–2077.
- (11) Silverman, A. I.; Boehm, A. B. Systematic Review and Meta-Analysis of the Persistence and Disinfection of Human Coronaviruses and Their Viral Surrogates in Water and Wastewater. *Environ. Sci. Technol. Lett.* **2020**, *7* (8), 544–553.
- (12) Kim, J. G.; Yousef, A. E.; Dave, S. Application of ozone for enhancing the microbiological safety and quality of foods: a review. *J. Food Prot.* **1999**, *62* (9), 1071–1087.
- (13) Wigginton, K. R.; Kohn, T. Virus disinfection mechanisms: the role of virus composition, structure, and function. *Curr. Opin. Virol.* **2012**, 2 (1), 84–89.
- (14) Ye, Y.; Chang, P. H.; Hartert, J.; Wigginton, K. R. Reactivity of Enveloped Virus Genome, Proteins, and Lipids with Free Chlorine and UV₂₅₄. *Environ. Sci. Technol.* **2018**, *52* (14), 7698–7708.
- (15) Vazquez-Bravo, B.; Goncalves, K.; Shisler, J. L.; Marinas, B. J. Adenovirus Replication Cycle Disruption from Exposure to Polychromatic Ultraviolet Irradiation. *Environ. Sci. Technol.* **2018**, *52* (6), 3652–3659.
- (16) Lee, J.; Zoh, K.; Ko, G. Inactivation and UV disinfection of murine norovirus with ${\rm TiO_2}$ under various environmental conditions. *Appl. Environ. Microbiol.* **2008**, *74* (7), 2111–2117.
- (17) Weng, S.; Dunkin, N.; Schwab, K. J.; McQuarrie, J.; Bell, K.; Jacangelo, J. G. Infectivity reduction efficacy of UV irradiation and peracetic acid-UV combined treatment on MS₂ bacteriophage and murine norovirus in secondary wastewater effluent. *J. Environ. Manage.* 2018, 221, 1–9.
- (18) Rockey, N.; Young, S.; Kohn, T.; Pecson, B.; Wobus, C. E.; Raskin, L.; Wigginton, K. R. UV Disinfection of Human Norovirus: Evaluating Infectivity Using a Genome-Wide PCR-Based Approach. *Environ. Sci. Technol.* **2020**, *54* (5), 2851–2858.

- (19) Lim, M. Y.; Kim, J. M.; Lee, J. E.; Ko, G. Characterization of ozone disinfection of murine norovirus. *Appl. Environ. Microbiol.* **2010**, 76 (4), 1120–1124.
- (20) Lim, M. Y.; Kim, J. M.; Ko, G. Disinfection kinetics of murine norovirus using chlorine and chlorine dioxide. *Water Res.* **2010**, 44 (10), 3243–3251.
- (21) Shin, G. A.; Sobsey, M. D. Inactivation of norovirus by chlorine disinfection of water. *Water Res.* **2008**, 42 (17), 4562–4568.
- (22) Ettayebi, K.; Crawford, S. E.; Murakami, K.; Broughman, J. R.; Karandikar, U.; Tenge, V. R.; Neill, F. H.; Blutt, S. E.; Zeng, X. L.; Qu, L.; Kou, B.; Opekun, A. R.; Burrin, D.; Graham, D. Y.; Ramani, S.; Atmar, R. L.; Estes, M. K. Replication of human noroviruses in stem cell-derived human enteroids. *Science* **2016**, *353* (6306), 1387–1393.
- (23) Santiana, M.; Ghosh, S.; Ho, B. A.; Rajasekaran, V.; Du, W. L.; Mutsafi, Y.; De Jesus-Diaz, D. A.; Sosnovtsev, S. V.; Levenson, E. A.; Parra, G. I.; Takvorian, P. M.; Cali, A.; Bleck, C.; Vlasova, A. N.; Saif, L. J.; Patton, J. T.; Lopalco, P.; Corcelli, A.; Green, K. Y.; Altan-Bonnet, N. Vesicle-Cloaked Virus Clusters Are Optimal Units for Inter-organismal Viral Transmission. *Cell Host Microbe* **2018**, 24 (2), 208–220.
- (24) Thorne, L. G.; Goodfellow, I. G. Norovirus gene expression and replication. *J. Gen. Virol.* **2014**, *95* (2), 278–291.
- (25) Flint, S. J. R., R, V..; Rall, G. F.; Skalka, A. M.; Enquist, L. W. *Principles of Virology*, 4 ed.; ASM Press: Washington, DC, 2015; Vol. 1., Molecular Biology.
- (26) Chen, Y. H.; Du, W.; Hagemeijer, M. C.; Takvorian, P. M.; Pau, C.; Cali, A.; Brantner, C. A.; Stempinski, E. S.; Connelly, P. S.; Ma, H. C.; Jiang, P.; Wimmer, E.; Altan-Bonnet, G.; Altan-Bonnet, N. Phosphatidylserine vesicles enable efficient *en bloc* transmission of enteroviruses. *Cell* **2015**, *160* (4), *619*–*630*.
- (27) Mutsafi, Y.; Altan-Bonnet, N. Enterovirus Transmission by Secretory Autophagy. *Viruses* **2018**, *10* (3), 139.
- (28) Altan-Bonnet, N.; Perales, C.; Domingo, E. Extracellular vesicles: Vehicles of en bloc viral transmission. *Virus Res.* **2019**, *265*, 143–149.
- (29) Akuma, P.; Okagu, O. D.; Udenigwe, C. C. Naturally Occurring Exosome Vesicles as Potential Delivery Vehicle for Bioactive Compounds. Frontiers in Sustainable Food Systems 2019, 3, 23.
- (30) Kumeda, N.; Ogawa, Y.; Akimoto, Y.; Kawakami, H.; Tsujimoto, M.; Yanoshita, R. Characterization of Membrane Integrity and Morphological Stability of Human Salivary Exosomes. *Biol. Pharm. Bull.* **2017**, *40* (8), 1183–1191.
- (31) Mirabelli, C.; Wobus, C. E. All Aboard! Enteric Viruses Travel Together. *Cell Host Microbe* **2018**, 24 (2), 183–185.
- (32) Young, D. C.; Sharp, D. G. Poliovirus aggregates and their survival in water. *Appl. Environ. Microbiol.* 1977, 33 (1), 168–177.
- (33) Hejkal, T. W.; Wellings, F. M.; Lewis, A. L.; LaRock, P. A. Distribution of viruses associated with particles in waste water. *Appl. Environ. Microbiol.* **1981**, *41* (3), 628–634.
- (34) Mattle, M. J.; Crouzy, B.; Brennecke, M.; Wigginton, K. R.; Perona, P.; Kohn, T. Impact of virus aggregation on inactivation by peracetic acid and implications for other disinfectants. *Environ. Sci. Technol.* **2011**, 45 (18), 7710–7717.
- (35) Thurston-Enriquez, J. A.; Haas, C. N.; Jacangelo, J.; Gerba, C. P. Chlorine inactivation of adenovirus type 40 and feline calicivirus. *Appl. Environ. Microbiol.* **2003**, *69* (7), 3979–85.
- (36) Wobus, C. E.; Thackray, L. B.; Virgin, H. W. t. Murine norovirus: a model system to study norovirus biology and pathogenesis. *J. Virol.* **2006**, *80* (11), 5104–5112.
- (37) Belliot, G.; Lavaux, A.; Souihel, D.; Agnello, D.; Pothier, P. Use of murine norovirus as a surrogate to evaluate resistance of human norovirus to disinfectants. *Appl. Environ. Microbiol.* **2008**, *74* (10), 3315–3318.
- (38) US EPA.Ultraviolet Disinfection Guidance Manual for the Final Long Term Enhanced Surface Water Treatment Rule, 2006.
- (39) Li, D.; Gu, A. Z.; He, M.; Shi, H. C.; Yang, W. UV inactivation and resistance of rotavirus evaluated by integrated cell culture and real-time RT-PCR assay. *Water Res.* **2009**, *43* (13), 3261–3269.

I

- (40) Romero-Maraccini, O. C.; Shisler, J. L.; Nguyen, T. H. Solar and temperature treatments affect the ability of human rotavirus wa to bind to host cells and synthesize viral RNA. *Appl. Environ. Microbiol.* **2015**, *81* (12), 4090–4097.
- (41) Levenson, E. A.; Martens, C.; Kanakabandi, K.; Turner, C. V.; Virtaneva, K.; Paneru, M.; Ricklefs, S.; Sosnovtsev, S. V.; Johnson, J. A.; Porcella, S. F.; Green, K. Y. Comparative Transcriptomic Response of Primary and Immortalized Macrophages to Murine Norovirus Infection. *J. Immunol.* **2018**, 200 (12), 4157–4169.
- (42) Bustin, S. A.; Benes, V.; Garson, J. A.; Hellemans, J.; Huggett, J.; Kubista, M.; Mueller, R.; Nolan, T.; Pfaffl, M. W.; Shipley, G. L.; Vandesompele, J.; Wittwer, C. T. The MIQE guidelines: minimum information for publication of quantitative real-time PCR experiments. Clin. Chem. 2009, 55 (4), 611–622.
- (43) Hwang, S.; Alhatlani, B.; Arias, A.; Caddy, S. L.; Christodoulou, C.; Bragazzi Cunha, J.; Emmott, E.; Gonzalez-Hernandez, M.; Kolawole, A.; Lu, J.; Rippinger, C.; Sorgeloos, F.; Thorne, L.; Vashist, S.; Goodfellow, I.; Wobus, C. E. Murine norovirus: propagation, quantification, and genetic manipulation. *Curr. Protoc Microbiol* **2014**, 33 (1), 15K.2.1–15K.2.61.
- (44) Blachere, F. M.; Lindsley, W. G.; McMillen, C. M.; Beezhold, D. H.; Fisher, E. M.; Shaffer, R. E.; Noti, J. D. Assessment of influenza virus exposure and recovery from contaminated surgical masks and N95 respirators. *J. Virol. Methods* **2018**, *260*, 98–106.
- (45) Darnell, M. E.; Subbarao, K.; Feinstone, S. M.; Taylor, D. R. Inactivation of the coronavirus that induces severe acute respiratory syndrome, SARS-CoV. *J. Virol. Methods* **2004**, *121* (1), 85–91.
- (46) Sokolova, V.; Ludwig, A. K.; Hornung, S.; Rotan, O.; Horn, P. A.; Epple, M.; Giebel, B. Characterisation of exosomes derived from human cells by nanoparticle tracking analysis and scanning electron microscopy. *Colloids Surf., B* **2011**, *87* (1), 146–150.
- (47) Bachurski, D.; Schuldner, M.; Nguyen, P. H.; Malz, A.; Reiners, K. S.; Grenzi, P. C.; Babatz, F.; Schauss, A. C.; Hansen, H. P.; Hallek, M.; Pogge von Strandmann, E. Extracellular vesicle measurements with nanoparticle tracking analysis An accuracy and repeatability comparison between NanoSight NS300 and ZetaView. *J. Extracell. Vesicles* 2019, 8 (1), 1596016.
- (48) Bolton, S. L.; Kotwal, G.; Harrison, M. A.; Law, S. E.; Harrison, J. A.; Cannon, J. L. Sanitizer efficacy against murine norovirus, a surrogate for human norovirus, on stainless steel surfaces when using three application methods. *Appl. Environ. Microbiol.* **2013**, 79 (4), 1368–1377.
- (49) Papahadjopoulos, D.; Jacobson, K.; Nir, S.; Isac, T. Phase transitions in phospholipid vesicles. Fluorescence polarization and permeability measurements concerning the effect of temperature and cholesterol. *Biochim. Biophys. Acta, Biomembr.* **1973**, *311* (3), 330–348.
- (50) Combes, G. B.; Varner, D. D.; Schroeder, F.; Burghardt, R. C.; Blanchard, T. L. Effect of cholesterol on the motility and plasma membrane integrity of frozen equine spermatozoa after thawing. *J. Reprod. Fertil., Suppl.* **2000**, No. 56, 127–132.
- (51) Cannon, J. L.; Aydin, A.; Mann, A. N.; Bolton, S. L.; Zhao, T.; Doyle, M. P. Efficacy of a levulinic acid plus sodium dodecyl sulfate-based sanitizer on inactivation of human norovirus surrogates. *J. Food Prot.* **2012**, *7*5 (8), 1532–1535.
- (52) Erickson, A. K.; Jesudhasan, P. R.; Mayer, M. J.; Narbad, A.; Winter, S. E.; Pfeiffer, J. K. Bacteria Facilitate Enteric Virus Coinfection of Mammalian Cells and Promote Genetic Recombination. *Cell Host Microbe* **2018**, 23 (1), 77–88.